Electrochimica Acta 117 (2014) 1–8

Contents lists available at ScienceDirect

Electrochimica Acta

journal homepage: www.elsevier.com/locate/electacta

Low temperature fabrication of high performance p-n junction on the Ti foil for use in large-area flexible dye-sensitized solar cells☆

Yaoming Xiao[a,b,*], Jihuai Wu[b,1], Jianming Lin[b], Miaoliang Huang[b], Leqing Fan[b], Zhang lan[b], Gaoyi Han[a], Sidian Li[a]

[a] Institute of Molecular Science, Shanxi University, Taiyuan 030006, P. R. China
[b] Institute of Materials Physical Chemistry, Huaqiao University, Quanzhou 362021, China

ARTICLE INFO

Article history:
Received 13 October 2013
Received in revised form
18 November 2013
Accepted 18 November 2013
Available online 1 December 2013

Keywords:
PEDOT
p-n junction
Dye-sensitized solar cell
Large-area
Low temperature

ABSTRACT

A p-n junction of poly (3,4-ethylenedioxythiophene) (PEDOT) - dye-sensitized TiO_2 is introduced into the large-area flexible dye-sensitized solar cell (DSSC) as an anode. This p-n junction is fabricated using a cyclic voltammetry electropolymerization of PEDOT onto a Ti foil substrate, and then treated in the aqueous ammonia, finally subjected to coating TiO_2 by a doctor-scraping technique, all of preparations and treatments are carried out under low temperature. The obtained p-n junction forms a single directional pathway for electron transport which benefites the charge separation. The large-area (10 cm^2) flexible DSSC with the p-n junction demonstrates an enhanced photovoltaic conversion efficiency of up to 6.51% compared to 4.89% for the DSSC without the p-n junction due to its low series resistance and charge-transfer resistance, high effective electron lifetime for recombination. As a result, the DSSC fabricated using the p-n junction can be suitable for high powered DSSC applications.

1. Introduction

Dye-sensitized solar cells (DSSCs) represent a low-cost alternative to conventional photovoltaic devices and have recently attracted much research interest [1], attributable to their easy fabrication, good stability, and high conversion efficiency [2–5]. In order to overcome some problems in general DSSCs in which TiO_2 porous films are solidified on a conductive glass substrate, flexible DSSCs based on metal foils or polymer substrates have attracted wide researches, due to their light weight, good flexibility, impact-proof, and low cost [6–8]. Besides, the flexible DSSC has been seen as the 3rd generation photovoltaic cell as well as the organic photovoltaic (OPV) device [9], owing to its shape or surface can be devised and constructed, and the technique of large-scale roll-to-roll (R2R) processing and rapid coating can be used in the flexible DSSC, which further decreases the cost and broadens the application for the flexible DSSC. Where the R2R process has been utilized for the industrial production of the OPV materials [10–12], and the OPV cell shows good operational stability under the consensus stability testing protocols (ISOS standards) [13] and reaches one-day energy pay-back for the factories [14]. Ti foils and Ti meshes have been utilized to manufacture large-area flexible DSSCs as anode and counter electrode materials, due to theirs flexibility and relatively low sheet resistance compared to those of the conducting glass substrate [15–17]. Ti-based materials have superior corrosion resistances in the contacting I_3^-/I^- electrolyte because of the passive oxide film of TiO_2 on these substrates.

As we have seen, the research of novel architectures and high performance flexible electrodes, such as that with a p-n junction structure, good electroconductivity, and excellent flexibility is still a challenge for the science development [18]. Looking for a suitable p-type hole transporting material which can match with the n-type semiconducting material of TiO_2 is a key issue to form a p-n junction in the flexible DSSC. Recently, Heng et al. reported a p-n junction of CuI-TiO_2 which was introduced to the flexible DSSC and showed an enhanced efficiency of 4.73% [19]. As extensively used p-type conducting polymers, e.g., polypyrrole [20,21], polyaniline [22,23], and poly (3,4-ethylenedioxythiophene) (PEDOT) [24–30], have received considerable attention in DSSCs. These p-type conducting polymers are advantageous over other small molecules owing to their low cost, good stability, and simple easy preparation of designable structures. Among them, PEDOT has already been reported as a cost-effective and stable counter electrode for catalyzing the reaction of I_3^-/I^- redox couple in DSSCs [24–26]. In addition,

* Corresponding author. Tel.: +86 351 7010699; fax: +86 351 7016358.
E-mail addresses: ymxiao2011@sohu.com (Y. Xiao), jhwu@hqu.edu.cn (J. Wu).
[1] Tel.: +86 595 22693899; fax: +86 595 22692229.

0013-4686/$ – see front matter © 2013 Elsevier Ltd. All rights reserved.
http://dx.doi.org/10.1016/j.electacta.2013.11.096

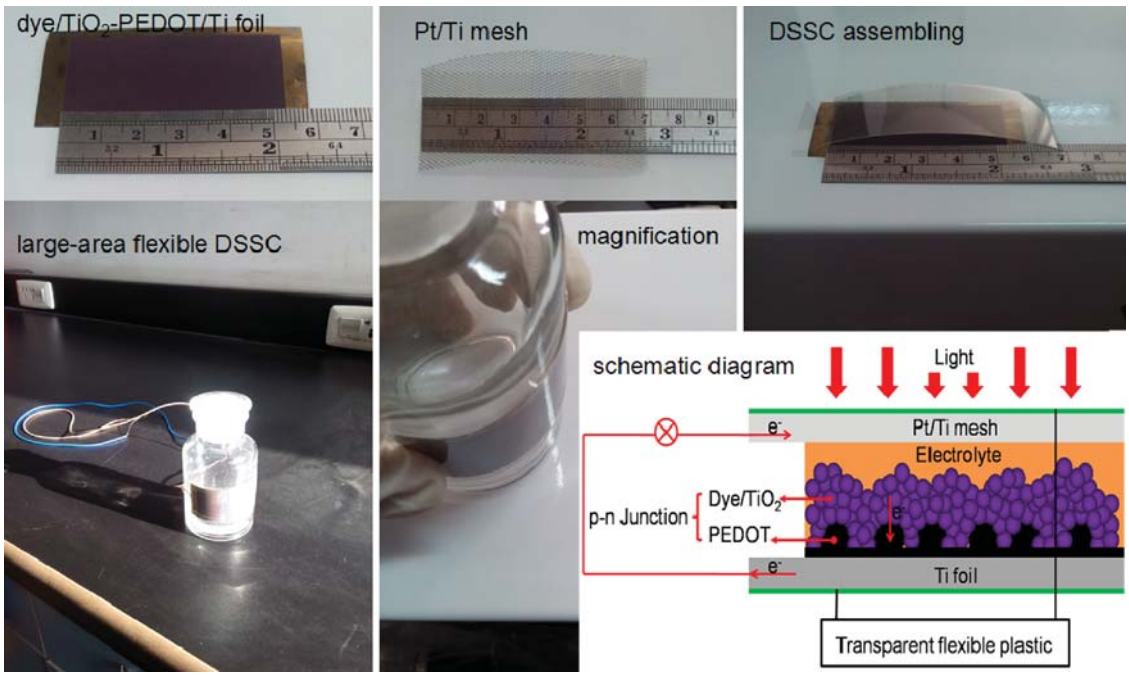

Fig. 1. Photographs and schematic diagram of the p-n junction based flexible dye-sensitized solar cell.

PEDOT is also potentially applicable as a hole transporting material in a solid-state DSSCs [27–30]. For instance, Koh et al. were successful at improving the power conversion efficiency significantly up to 6.80% by using PEDOT, and the active area of the DSSC was 0.16 cm^2 [30].

In this paper, integrating the merits of the Ti-based substrates and PEDOT, we report on low temperature fabrication a new p-n junction of dye-sensitized TiO_2-PEDOT/Ti and using in a large-area flexible DSSC with an active area of 10 cm^2 (shown in Fig. 1).

2. Experimental

2.1. Materials

3, 4-ethylenedioxythiophene monomer (EDOT) was purchased from Aldrich, USA. Sodium dodecyl sulfate (SDS), lithium pechlorate ($LiClO_4$), aqueous ammonia, hydrofluoric acid, ethanol, iodine, lithium iodide, tetrabutyl ammonium iodide, 4-tert-butyl-pyridine, and acetonitrile were purchased from Shanghai Chemical Agent Ltd., China (Analysis purity grade). Titania nanopowder (P25) was purchased from Degussa, Germany. Sensitized-dye N719 [cis-di(thiocyanato)-N,N′-bis (2,2′-bipyridyl-4-carboxylic acid-4-tetrabutylammonium carboxylate) ruthenium (II)] was purchased from Dyesol, Australia. The above agents were used without further purification.

2.2. Fabrication of the flexible p-n junction

PEDOT was electrodeposited on the Ti foil by the cyclic voltammetry (CV) measurement from an aqueous solution containing 2.0 mM EDOT, 10 mM SDS, and 10 mM $LiClO_4$. A three-electrode cell with an Electrochemical Workstation (CHI660D, Shanghai Chenhua Device Company, China), comprised of the Ti foil (0.03 mm thickness, purchased from Baoji Yunjie Metal Production Co., Ltd., China) working electrode, a Pt wire counter electrode, and an Ag/AgCl reference electrode was used. Before the plating, Ti foil samples with rectangular dimension of 2.5 cm × 5.5 cm were cleaned with mild detergent and rinsed in distilled water. The Ti foil samples then immersed in hydrofluoric acid solution with suitable concentration for 2 min and rinsed in distilled water again. The cleaned Ti foil was designated as sample A. The CV plating PEDOT on the cleaned Ti foil was carried out at a "High E" of 1.1 V. The value of "Init E" was same as the "Low E", the CV parameters were shown in Fig. 2 in detail. For comparison, the value of "Sweep Segments" was changed, and the samples plated under "Sweep Segments" = 15, 30, and 45 were designated as sample B, C, and D, respectively. The obtained PEDOT/Ti samples were rinsed in distilled water and then immersed in an aqueous ammonia for 12 h to change their conductive state to semiconductor state. Finally, the samples were drying at 80 °C in a vacuum drying oven (Suzhou Jiangdong Precision Instrument Co., Ltd., China).

The TiO_2 colloid (prepared according to our previous report [31]) was coated on the cleaned Ti foil and different PEDOT/Ti samples using a doctor-scraping technique, respectively. The thickness of

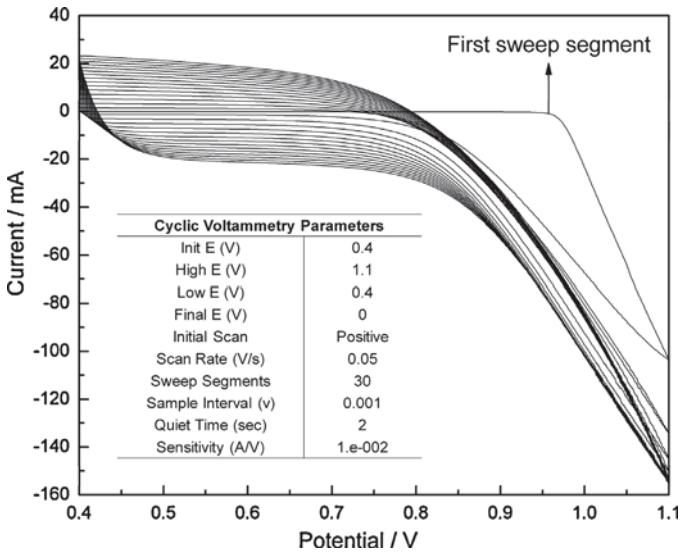

Fig. 2. Cyclic voltammetry for the electrodeposition of PEDOT on the Ti foil.

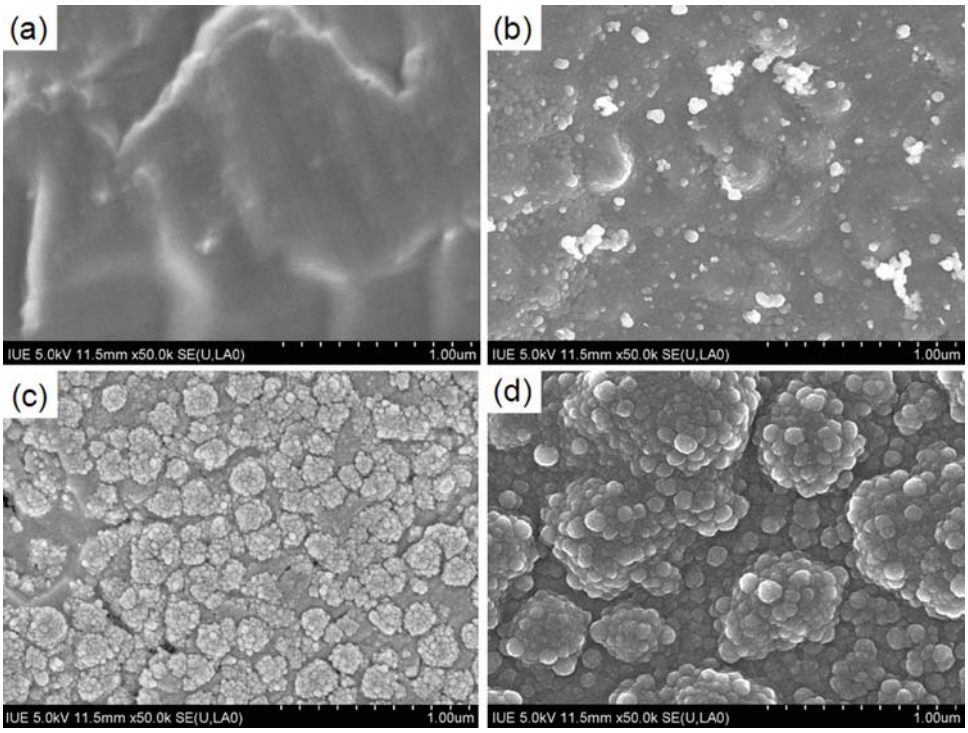

Fig. 3. SEM images of sample A (a), B (b), C (c), and D (d), respectively.

the TiO_2 film was controlled by the thickness of the adhesive tape around the edge of the cleaned Ti foil or PEDOT/Ti foil [32–34]. The process was repeated for three times to form a TiO_2 film with thickness of about 12 μm. The resultant TiO_2/Ti and TiO_2-PEDOT/Ti flexible films were heated at 100 °C for 30 min in the vacuum drying oven. Finally, the TiO_2/Ti and TiO_2-PEDOT/Ti flexible films were immersed in a 3.0×10^{-4} M dye N719 absolute ethanol solution for 24 h to absorb the dye adequately. Thus the dye-sensitized TiO_2/Ti and TiO_2-PEDOT/Ti flexible electrodes were obtained.

2.3. Assemblage of flexible DSSCs

The Pt/Ti counter electrodes were prepared on the Ti mesh substrates according to our previous reports under low temperature [16,35]. The large-area flexible DSSC with an active area of 2.0 cm × 5.0 cm was assembled by injection of a redox-active electrolyte into the aperture between the TiO_2-PEDOT/Ti anode and the Pt/Ti mesh counter electrode (as shown in Fig. 1). The two electrodes were clipped together with two transparent flexible plastics and a cyanoacrylate adhesive was used as a sealant to prevent the electrolyte solution from leaking. Epoxy resin was used to further seal the cell in order to enhance the cell stability. The redox electrolyte consisted of 0.60 M tetrabutyl ammonium iodide, 0.10 M lithium iodide, 0.10 M iodine, and 0.50 M 4-tert-butyl-pyridine in acetonitrile.

2.4. Characterization

The surface features of PEDOTs and TiO_2 anodes were observed using a scanning electron microscope (SEM, Hitachi S-4800, Japan). Fourier transform infrared spectra (FTIR) of samples were recorded on an Infrared Spectrometric Analyzer (Nicolet Impact 410 spectrometer, Japan) using KBr as pellets. Electrochemical impedance spectroscopy (EIS) measurements of the flexible DSSCs were carried out using a Zahner electrochemical workstation. The symmetric dummy cells were used for impedance studies. The impedance studies were carried out simulating open-circuit conditions at ambient atmosphere, and the impedance data covered a frequency range of 10^{-1}-10^{6} Hz with zero bias potential and 10 mV of amplitude, under a dark condition. The resultant impedance spectra were analyzed by means of the Z-view software. The reflectivity of the flexible TiO_2 anode was carried out with an ultraviolet-visible spectrophotometer (UV-2550, Shimadzu, Japan). The dye adsorbed on the anode was determined by measuring the dye amount released in the solution of 5 ml 0.05 M NaOH. The measurement was carried out with an ultraviolet-visible spectrometer (UV-2800H, UNICO (Shanghai) Instruments Co., Ltd.). The incident monochromatic photon-to-current conversion efficiency (IPCE) curves were measured with a Newport Monochromator (Power Meter Model 2936-C, Newport Corporation, U. S. A.).

2.5. Photoelectrochemical measurements

The photocurrent density-voltage (*J-V*) characteristics were made using a computer-controlled Keithley 2400 source meter under illumination by a solar simulator (Yamashita Denso YSS-150A). The incident light intensity and the active cell area were 100 mW·cm^{-2} (AM 1.5) and 10 cm^2, respectively. The photoelectronic performances [i.e. fill factor (*FF*) and overall energy conversion efficiency (η)] were calculated by the following equations [36]:

$$FF = \frac{V_{max} \times J_{max}}{V_{oc} \times J_{sc}} \quad (1)$$

$$\eta\ (\%) = \frac{V_{max} \times J_{max}}{P_{in}} \times 100\% = \frac{V_{oc} \times J_{sc} \times FF}{P_{in}} \times 100\% \quad (2)$$

where J_{SC} is the short-circuit current density (mA·cm^{-2}), V_{OC} is the open-circuit voltage (V), P_{in} is the incident light power, and J_{max} (mA·cm^{-2}) and V_{max} (V) are the current density and voltage in the *J-V* curves, respectively, at the point of maximum power output.

Table 1
EIS results of flexible DSSCs based on sample A (without p-n junction) and C (with p-n junction).

sample	R_S ($\Omega\cdot cm^2$)	$R_{CT}(Pt)$ ($\Omega\cdot cm^2$)	$R_{CT}(TiO_2)$ ($\Omega\cdot cm^2$)	$Y_{CPE}(Pt)$ ($mF\cdot cm^{-2}$)	$Y_{CPE}(TiO_2)$ ($mF\cdot cm^{-2}$)	W ($\Omega\cdot cm^2$)	ω_{min} (Hz)	τ_r (ms)
A	6.51	1.29	3.54	1.14	1.01	7.89	3296	0.30
C	6.36	1.27	2.14	1.17	1.57	4.40	2087	0.48

3. Results and discussion

3.1. Morphology and composition of different PEDOTs

Fig. 3 represents the SEM images of the sample A, B, C, and D, respectively. It can be found that the surface of the cleaned Ti foil was roughened slightly after immersed in the hydrofluoric acid solution. According to Fig. 3b, c, and d, it is obvious that the PEDOT was grown up with increasing the sweep segments, and Fig. 3c illustrates that the PEDOT with a size diameter of about 100-200 nm was electrodeposited on the Ti foil.

Fig. 4 demonstrates the FTIR spectra of different PEDOTs. The signals in these three spectra are almost the same. The vibrations at 1515 and 1337 cm^{-1} can be owing to the C=C and C-C stretching of the quinoidal structure of the thiophene ring. The vibrations at 1203, 1142 and 1091 cm^{-1} are possibility attributed to C-O-C bond stretching in the ethylene dioxy group. The C-S bond stretching in the thiophene ring is also found at 980, 845, and 693 cm^{-1} [37,38]. The FTIR spectra therefore prove that the PEDOT thin films were successfully electrodeposited on Ti foil substrates by using the cyclic voltammetry method.

3.2. Influence of different anodes on the morphology and resistance

Fig. 5a and b show the SEM images of flexible anodes prepared on the sample A and C, respectively. The inset of Fig. 5a represents the cross-sectional image of TiO_2 film with a thickness of about 12 μm. Compared to the two flexible anodes, the anode prepared on PEDOT/Ti foil have a larger void space to harvest more light. Fig. 5c shows the possible mechanism of the DSSC with the p-n junction. In the traditional DSSC, the conductive band (CB) of semiconductor TiO_2 collects the photon-generated electrons from the excited dye molecules (D*) under sunlight. The most part of the collected electrons in the CB of TiO_2 can be exported by the conducting glass, and forming the photo-current by the external circuit. However, the rest is wasted by the electron recombination to dye molecules and electron back reaction with electrolyte [39]. In order to suppress the above-mentioned electron recombination and electron back reaction, a p-n junction can be used by introducing a PEDOT layer to the DSSC (shown in Fig. 1). As we all know, the p-n junction can supply a single directional electron transmission from the n-type to the p-type, but the backward transmission is prohibited. Therefore, the directional electron transmission will benefit the charge separation, resulting in quick and efficient transport for electrons in the film, and enhancing the efficiency of the flexible DSSC [19,29,30].

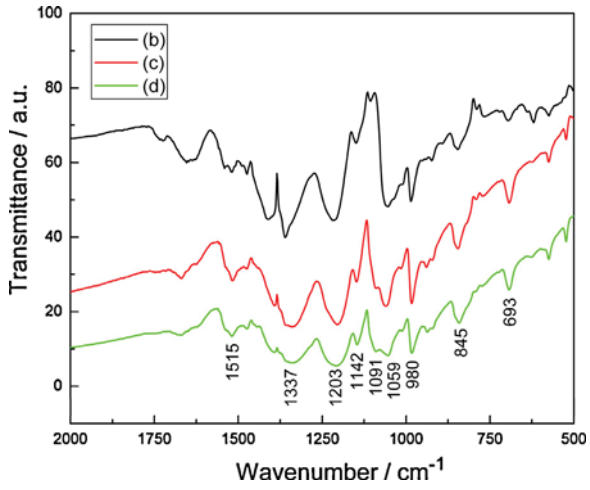

Fig. 4. FTIR spectra of PEDOTs based on sample B (b), C (c), and D (d), respectively.

Electrochemical impedance spectroscopy (EIS) was used to characterize the internal resistance and charge transfer kinetics of p-n junction [40,41], as shown in Fig. 6. The equivalent circuit of this model (inset of Fig. 6a) has been already reported [29,30,42]. The intercept of the real axis at high frequency is the ohmic series resistance (R_S) including the sheet resistance of the anode, the counter electrode, and the electrolytic resistance. The first semicircle at high frequency refers to the $R_{CT}(Pt)$ for the charge-transfer resistance at the counter electrode/electrolyte interface, while the second semicircle at middle frequency refers to the $R_{CT}(TiO_2)$ for the charge-transfer resistance at the electrolyte/anode interface [43], and the third semicircle at low frequency represents the Nernst diffusion impedance (W) corresponding to the diffusion resistance of the I^-/I_3^- redox species. The constant phase elements ($Y_{CPE}(Pt)$ and $Y_{CPE}(TiO_2)$) are frequently used as substitutes for the capacitors in an equivalent circuit to fit the impedance behavior of the electrical double layer more accurately while the double layer does not behave as an ideal capacitor [43].

The results of the impedance data are shown in Table 1. It can be seen that the two kinds of DSSCs have similar values of $R_{CT}(Pt)$ and $Y_{CPE}(Pt)$, this is because of the two kinds of cells have same Pt counter electrode and electrolyte. However, the R_S values are different, owing to the different anodes. The DSSC fabricated with the p-n junction exhibits a lower $R_{CT}(TiO_2)$, indicating lower resistance to charge transport between the electrolyte and the TiO_2-PEDOT/Ti anode. In addition, a larger $Y_{CPE}(TiO_2)$ of the TiO_2-PEDOT/Ti anode corresponds to its larger surface area, which can improve the dye absorption and harvest more light. Additionally, the Nernst diffusion impedance for the DSSC with the p-n junction demonstrates a lower W, which reveals that the diffusion of I_3^- in the TiO_2-PEDOT/Ti anode is easier. Based on the EIS model, the effective electron lifetime for recombination (τ_r) in the anode can be calculated from the minimum angular frequency (ω_{min}) value by the following equation: $\tau_r = 1/\omega_{min}$, where the ω_{min} values come from the impedance semicircle at middle frequencies in the Bode spectrum. The τ_r value for the flexible DSSC with the p-n junction has a higher value of 0.48 ms. This could effectively decrease the electron recombination, resulting in significantly enhanced the electron transfer and further improved the cell performance [19,29,30].

3.3. Influence of different anodes on the reflectivity and dye adsorption

Fig. 7 shows the reflectance and dye absorption spectra of flexible dye-sensitized TiO_2 anodes prepared on the sample A and C, respectively. From Fig. 7a, the wavelength at 530 nm comes from the dye absorption [44], the reflectance of the anode with the p-n junction is lower than that of the anode without the p-n junction. One possible explanation is the surface of the cleaned Ti foil is flat with little rough, and this structure leads to a higher reflectance. The anode based on the p-n junction with a special surface of PEDOT could be used to catch the light, resulting in a smaller reflectance.

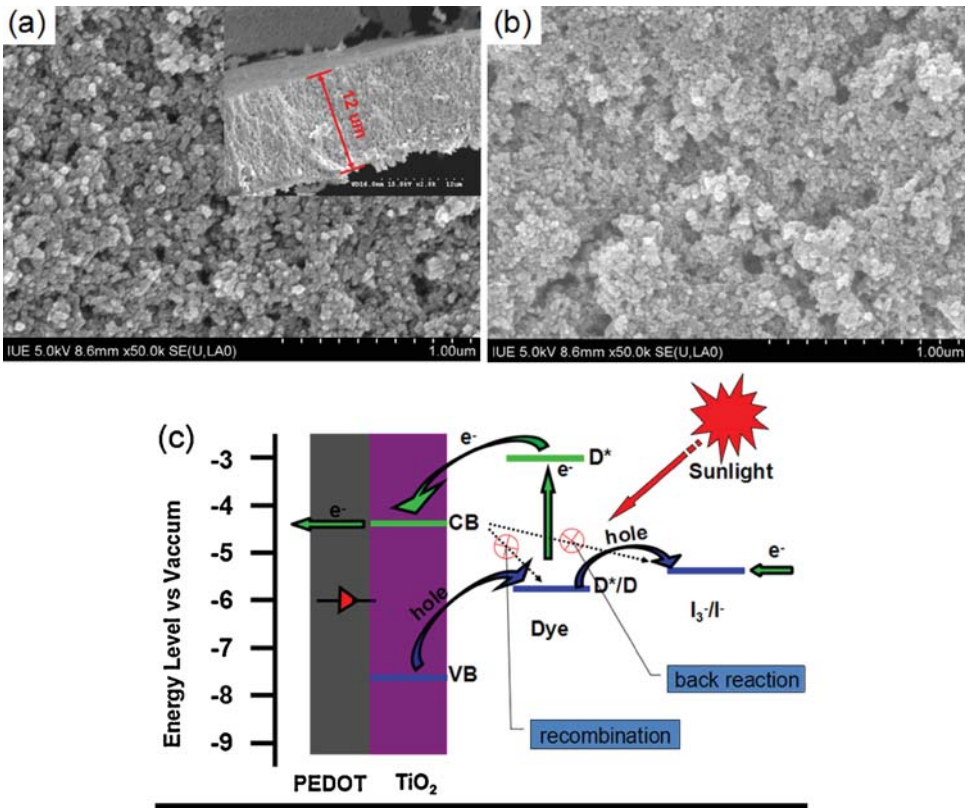

Fig. 5. SEM images of TiO_2/Ti based on sample A (a) and TiO_2-PEDOT/Ti based on sample C (b), schematic of the mechanism of the p-n junction (c); Cross-sectional SEM image of TiO_2/Ti (inset of Fig. 5a).

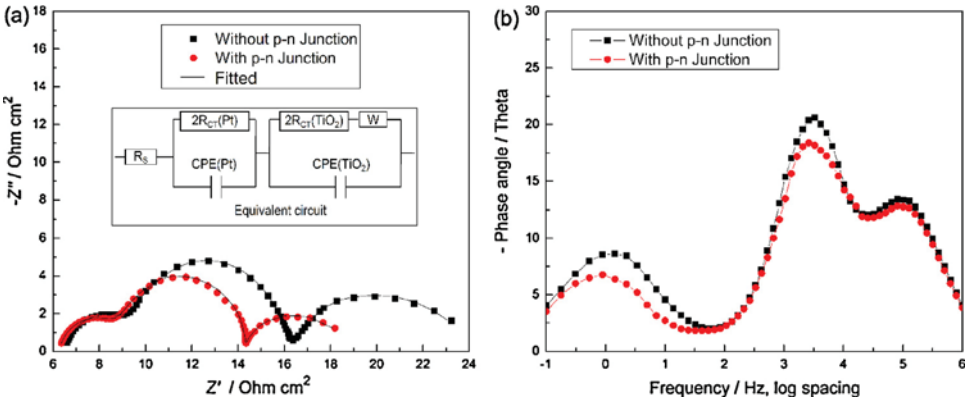

Fig. 6. Nyquist plots (a) and Bode phase plots (b) of flexible DSSCs based on sample A (without p-n junction) and C (with p-n junction); Inset (a) is the equivalent circuit of the large-area flexible DSSC.

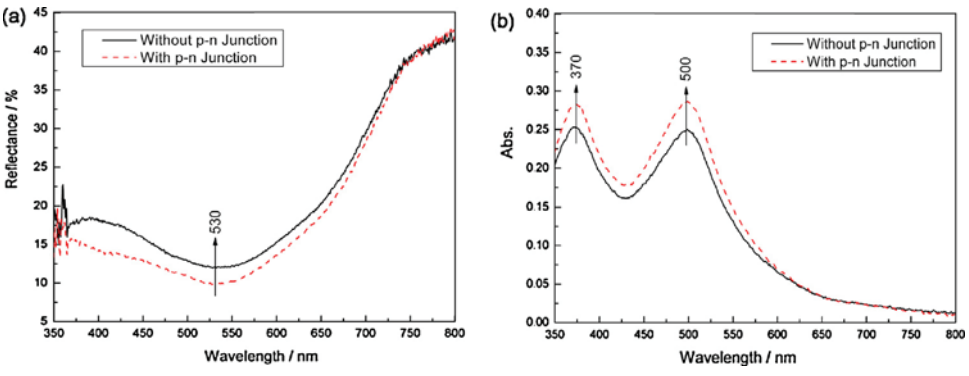

Fig. 7. Reflectance (a) and dye adsorption (b) of the dye-sensitized TiO_2 anodes based on sample A (without p-n junction) and C (with p-n junction).

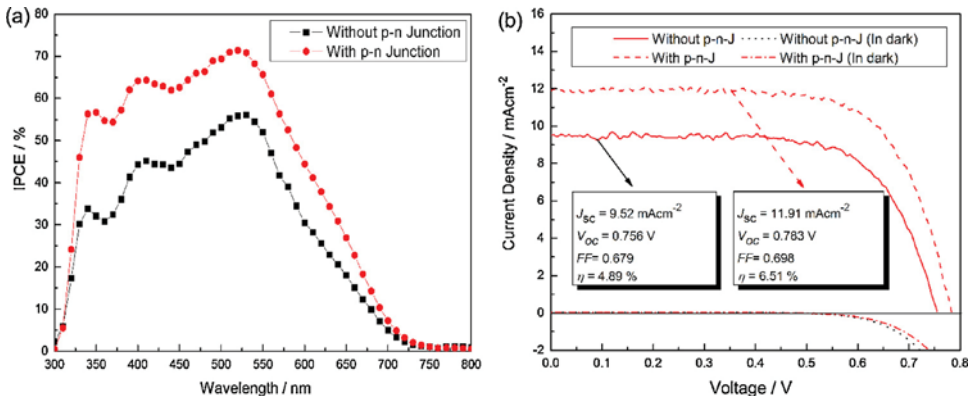

Fig. 8. IPCE (a) and *J-V* curves (under light intensity of 100 mW·cm^{-2} and in the dark) (b) of flexible DSSCs based on sample A (without p-n junction) and C (with p-n junction).

The lower reflectance means that less light is reflected off the space and more light is utilized. Other reason may be attributed to the different dye adsorption of the two kinds of anodes. In Fig. 7b, the absorption peaks at 370 nm and 500 nm come from the dye absorption and blue-shift in the alkali solution [44], the absorbance for the anode with the p-n junction is the higher than that of the anode without the p-n junction, which results in a more adsorption for the dye. According to the Lambert-Beer's law, higher absorbance means the higher dye concentration. It is well-known that the photocurrent of the DSSC is directly correlated with the amount of the dye molecule, the more dye molecules are adsorbed, the more incident light is harvested, and the larger photocurrent occurs. According to our experiments, the flexible anode prepared on the PEDOT/Ti can harvest more light and produce larger photocurrent.

3.4. Photovoltaic properties

Fig. 8a demonstrates the IPCE curves of the flexible DSSCs based on the anode with and without the p-n junction respectively. It is noticeable that the IPCE curve for the flexible DSSC using the TiO_2-PEDOT/Ti anode from 350 nm to 700 nm is higher than that for the TiO_2/Ti anode, resulting in a difference in J_{SC}. Fig. 8b shows the *J-V* curves of flexible DSSCs with and without the p-n junction under light intensity of 100 mW·cm^{-2} (above) and in the dark (below), respectively. As shown in Fig. 8b, the J_{SC} and V_{OC} values of the flexible DSSC with the p-n junction are higher than those of the DSSC without the p-n junction. This is due to the difference of the reflectance and dye absorption of flexible anodes, and the effect of electron transport of the p-n junction. On the one hand, the flexible anode prepared on the PEDOT/TiO_2 has lower reflectance and higher dye absorption, which can harvest more light and produce larger photocurrent [45]. On the other hand, the TiO_2-PEDOT/Ti anode can work as a high performance p-n junction to provide a single directional pathway for electron transport which benefits the charge separation, thereby enhancing the efficiency of the flexible DSSC [19,29,30]. Moreover, the fill factor (*FF*) value of the DSSC with the p-n junction is higher than that of the DSSC without the p-n junction, this is owing to the values of R_S, $R_{CT}(TiO_2)$ and *W* of the former are lower than those of the latter [42,46]. Fig. 8b also shows the dark current-voltage characteristics of the corresponding photocurrent-voltage curves (below). It is obvious that the voltage of DSSC with the p-n junction is higher than that without the p-n junction, which indicates that the internal consumption of current is lower, leading to the high open-circuit voltage [47]. Therefore, the η value of the DSSC with the p-n junction shows higher than that of the DSSC without the p-n junction.

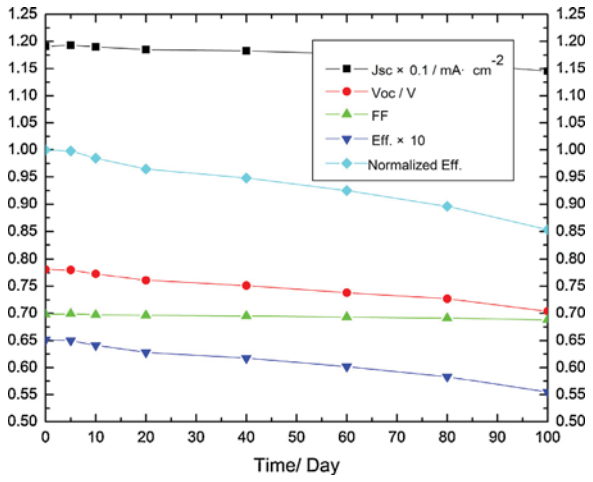

Fig. 9. Time-course changes of the normalized efficiency and photovoltaic performances of the large-area flexible DSSC based on sample C (with p-n junction), under light intensity of 100 mW·cm^{-2}.

Fig. 9 shows the the operational stability of the large-area flexible DSSC based on sample C (with p-n junction) under light intensity of 100 mW·cm^{-2}. As a whole, the photovoltaic performances and normalized efficiency decrease with the continuation of time. However, the efficiency (η) of the device reduces from 6.51% to 5.55% after 100 days, thereby 85.3 percent of the energy conversion efficiency is kept, indicating the device has a good long-term stability.

The photovoltaic properties of flexible DSSCs based on different TiO_2-PEDOT/Ti anodes were also measured under irradiation with a light intensity of 100 mW·cm^{-2}, and the results were summarized in Table 2. As shown, the J_{SC} values increase firstly and then decrease with the increase of the values of sweep segments, this may be the proper size diameter of the PEDOT particles can reduce the reflectance, increase the dye absorption, and enhance the effect of electron transport of the anode. It can be found that these DSSCs based on different TiO_2-PEDOT/Ti anodes have comparatively similar V_{OC} (0.783 V). This can be owing to the V_{OC} is mainly determined

Table 2
The photovoltaic performance of DSSCs with different photoanodes prepared at a "Sweep Segments" of 15, 30, and 45, respectively.

sample	Sweep Segments	J_{SC} (mA·cm^{-2})	V_{OC} (V)	*FF*	η (%)
B	15	10.47	0.781	0.691	5.65
C	30	11.91	0.783	0.698	6.51
D	45	11.26	0.783	0.697	6.15

by the energy level difference between the Fermi level of the electron in anode and the redox potential of the electrolyte [1,2], since these flexible DSSCs have the same compositions, their V_{OC} are close. The fill factor (*FF*) values are slightly changed with the enlargement the values of sweep segments. Therefore, the η values of the DSSC increases firstly and then decreases with increasing the values of the sweep segments, and the η value of 6.51% was reached for the large-area (active area of 10 cm^2) flexible DSSC with p-n junction, under a light irradiation with an intensity of 100 $mW{\cdot}cm^{-2}$.

4. Conclusion

In summary, a p-type hole transporting material PEDOT with a size diameter of about 100-200 nm was electrodeposited onto the Ti foil using a cyclic voltammetry method at 30 sweep segments, which had optimum feature and high performance compared to the other sweep segments preparation PEDOT/Ti. Then coating TiO_2 onto the PEDOT/Ti to form a p-n junction using in the large-area flexible DSSC as an anode. The obtained high performance p-n junction formed a single directional pathway for electron transport which benefited the charge separation and improved the efficiency of the flexible DSSC as a result. This DSSC based on the p-n junction showed low series resistance of 6.36 $\Omega{\cdot}cm^2$, charge-transfer resistance ($R_{CT}(TiO_2)$) of 2.14 $\Omega{\cdot}cm^2$, and higher effective electron lifetime for recombination of 0.48 ms. The light-to-electric energy conversion efficiency of the large-area (10 cm^2) flexible DSSC with the p-n junction demonstrated an enhanced photovoltaic conversion efficiency of up to 6.51% compared to 4.89% for the DSSC without the p-n junction, and reduced from 6.51% to 5.55% after 100 days, thereby 85.3 percent of the energy conversion efficiency was kept, indicating the device had a good long-term stability. Based on this result, the DSSC fabricated using the p-n junction is suitable for high powered DSSC applications.

Acknowledgments

The authors acknowledeg the financial joint support by the National Natural Science Foundation of China (Nos. U1205112, 50842027) and the special research fund for the doctoral program of Higher University, Ministry of Education, China (No. 20123501110001).

References

[1] B. O' Regan, M. Grätzel, Low-cost high-efficiency solar cell based on dye-sensitized colloidal TiO_2 films, Nature 353 (1991) 737.
[2] M. Grätzel, Solar energy conversion by dye-sensitized photovoltaic cells, Inorg. Chem. 44 (2005) 6841.
[3] M. Grätzel, Recent advances in sensitized mesoscopic solar cells, Accounts Chem. Res. 42 (2009) 1788.
[4] L. Han, As. Islam, H. Chen, C. Malapaka, B. Chiranjeevi, S. Zhang, X. Yang, M. Yanagida, High-efficiency dye-sensitized solar cell with a novel co-adsorbent, Energy Environ. Sci. 5 (2012) 6057.
[5] J. Burschka, N. Pellet, S. Moon, R. Humphry-Baker, P. Gao, M. Nazeeruddin, M. Grätzel, Sequential deposition as a route to high-performance perovskite-sensitized solar cells, Nature 499 (2013) 316.
[6] H. Lindstrom, A. Holmberg, E. Magnusson, L. Malmqvist, A. Hagfeldt, A new method to make dye-sensitized nanocrystalline solar cells at room temperature, J. Photochem. Photobio. A 145 (2001) 107.
[7] C. Longo, J. Freitas, M. DePaoli, Performance and stability of TiO_2/dye solar cells assembled with flexible electrodes and a polymer electrolyte, J. Photochem. Photobio. A 159 (2003) 33.
[8] S. Ito, N. Ha, G. Rothenberger, P. Liska, P. Comte, S. Zakeeruddin, P. Péchy, M. Nazeeruddin, M. Grätzel, High-efficiency (7.2%) flexible dye-sensitized solar cells with Ti-metal substrate for nanocrystalline-TiO_2 photoanode, Chem. Commun. 38 (2006) 4004.
[9] F. Krebs, J. Fyenbo, D. Tanenbaum, S. Gevorgyan, R. Andriessen, B. Remoortere, Y. Galagand, M. Jørgensen, The OE-A OPV demonstrator anno domini 2011, Energy Environ. Sci. 4 (2011) 4116.
[10] F. Krebs, T. Tromholt, M. Jørgensen, Upscaling of polymer solar cell fabrication using full roll-to-roll processing, Nanoscale 2 (2010) 873.
[11] D. Angmo, T. Larsen-Olsen, M. Jørgensen, R. Søndergaard, F. Krebs, Roll-to-roll inkjet printing and photonic sintering of electrodes for ITO free polymer solar cell modules and facile product integration, Adv. Energy. Mater. 3 (2013) 172.
[12] F. Krebs, M. Hösel, M. Corazza, B. Roth, M. Madsen, S. Gevorgyan, R. Søndergaard, D. Karg, M. Jørgensen, Freely available OPV—The fast way to progress, Energy Tech. 1 (2013) 378.
[13] M. Reese, S. Gevorgyan, M. Jørgensen, E. Bundgaard, S. Kurtz, D. Ginley, D. Olson, M. Lloyd, P. Morvillo, E. Katz, A. Elschner, O. Haillant, T. Currier, V. Shrotriya, M. Hermenau, M. Riede, K. Kirov, G. Trimmel, T. Rath, O. Inganäs, F. Zhang, M. Andersson, K. Tvingstedt, M. Lira-Cantu, D. Laird, C. McGuiness, S. Gowrisanker, M. Pannone, M. Xiao, J. Hauch, R. Steim, D. DeLongchamp, R. Rösch, H. Hoppe, N. Espinosa, A. Urbina, G. Yaman-Uzunoglu, J. Bonekamp, A. Breemen, C. Girotto, E. Voroshazi, F. Krebs, Consensus stability testing protocols for organic photovoltaic materials and devices, Sol. Energy Mater. Sol. Cells 95 (2011) 1253.
[14] N. Espinosa, M. Hösel, D. Angmo, F. Krebs, Solar cells with one-day energy payback for the factories of the future, Energy Environ. Sci. 5 (2012) 5117.
[15] Y. Xiao, J. Wu, G. Yue, J. Lin, M. Huang, L. Fan, Z. Lan, Fabrication of high performance Pt/Ti counter electrodes on Ti mesh for flexible large-area dye-sensitized solar cells, Electrochimica Acta 58 (2011) 621.
[16] Y. Xiao, J. Wu, G. Yue, J. Lin, M. Huang, L. Fan, Z. Lan, The surface treatment of Ti meshes for use in large-area flexible dye-sensitized solar cells, J. Power Sources 208 (2012) 197.
[17] J. Wu, Y. Xiao, G. Yue, Q. Tang, J. Lin, M. Huang, Y. Huang, L. Fan, Z. Lan, S. Yin, T. Sato, A large-area light-weight dye-sensitized solar cell based on all titanium substrates with an efficiency of 6.69% outdoors, Adv. Mater. 24 (2012) 1884.
[18] Y. Zhang, H. Dong, Q. Tang, S. Ferdous, F. Liu, S. Mannsfeld, W. Hu, A. Briseno, Organic single-crystalline p-n junction nanoribbons, J. Am. Chem. Soc. 132 (2010) 11580.
[19] L. Heng, X. Wang, N. Yang, J. Zhai, M. Wan, L. Jiang, p-n-junction-based flexible dye-sensitized solar cells, Adv. Funct. Mater. 20 (2010) 266.
[20] J. Wu, Q. Li, L. Fan, Z. Lan, P. Li, J. Lin, S. Hao, High-performance polypyrrole nanoparticles counter electrode for dye-sensitized solar cells, J. Power Sources 181 (2008) 172.
[21] Y. Guo, Y. Zhang, H. Liu, S. Lai, Y. Li, Y. Li, W. Hu, S. Wang, C. Che, D. Zhu, Assembled organic/inorganic p-n junction interface and photovoltaic cell on a single nanowire, J. Phys. Chem. Lett. 1 (2010) 327.
[22] J. Gong, Y. Li, Z. Hu, Z. Zhou, Y. Deng, Ultrasensitive NH_3 gas sensor from polyaniline nanograin enchased TiO_2 fibers, J. Phys. Chem. C 114 (2010) 9970.
[23] K. Huang, J. Huang, C. Wu, C. Liu, H. Chen, C. Chu, J. Lin, C. Lin, K. Ho, Nanographite/polyaniline composite films as the counter electrodes for dye-sensitized solar cells, J. Mater. Chem. 21 (2011) 10384.
[24] J. Pringle, V. Armel, D. MacFarlane, Electrodeposited PEDOT-on-plastic cathodes for dye-sensitized solar cells, Chem. Commun. 46 (2010) 5367.
[25] Y. Xiao, J. Lin, S. Tai, S. Chou, G. Yue, J. Wu, Pulse electropolymerization of high performance PEDOT/MWCNT counter electrodes for Pt-free dye-sensitized solar cells, J. Mater. Chem. 22 (2012) 19919.
[26] Y. Xiao, J. Wu, J. Lin, G. Yue, J. Lin, M. Huang, Z. Lan, L. Fan, A dual function of high performance counter electrode for stable quasi-solid-state dye-sensitized solar cells, J. Power Sources 241 (2013) 373.
[27] J. Xia, N. Masaki, N. Lira-Cantu, Y. Kim, K. Jiang, S. Yanagida, Influence of doped anions on poly (3, 4-ethylenedioxythiophene) as hole conductors for iodine-free solid-state dye-sensitized solar cells, J. Am. Chem. Soc. 130 (2008) 1258.
[28] K. Jiang, K. Manseki, Y. Yu, N. Masaki, K. Suzuki, Y. Song, S. Yanagida, Photovoltaics based on hybridization of effective dye-sensitized titanium oxide and hole-conductive polymer P3HT, Adv. Funct. Mater. 19 (2009) 2481.
[29] J. Kim, J. Koh, B. Kim, S. Ahn, H. Ahn, D. Ryu, J. Kim, E. Kim, Enhanced performance of I_2-free solid-state dye-sensitized solar cells with conductive polymer up to 6.8%, Adv. Funct. Mater. 21 (2011) 4633.
[30] J. Koh, J. Kim, B. Kim, J. Kim, E. Kim, Highly efficient, iodine-free dye-sensitized solar cells with solid-state synthesis of conducting polymers, Adv. Mater. 23 (2011) 1641.
[31] Y. Xiao, J. Wu, G. Yue, G. Xie, J. Lin, M. Huang, The preparation of titania nanotube and its application in flexible dye-sensitized solar cells, Electrochimica Acta 55 (2010) 4573.
[32] J. Wu, Z. Lan, J. Lin, M. Huang, S. Hao, T. Sato, S. Yin, A novel thermosetting gel electrolyte for stable quasi-solid-state dye- sensitized solar cells, Adv. Mater. 19 (2007) 4006.
[33] J. Wu, S. Hao, Z. Lan, J. Lin, M. Huang, Y. Huang, P. Li, S. Yin, T. Sato, An all-solid-state dye-sensitized solar cell-based poly(N-alkyl-4-vinyl- pyridine iodide) electrolyte with efficiency of 5.64%, J. Am. Chem. Soc. 130 (2008) 11568.
[34] Z. Lan, J. Wu, S. Hao, J. Lin, M. Huang, Y. Huang, Template-free synthesis of closed-microporous hybrid and its application in quasi-solid-state dye-sensitized solar cells, Energy Environ. Sci. 2 (2009) 524.
[35] Y. Xiao, J. Wu, G. Yue, J. Lin, M. Huang, Z. Lan, Low temperature preparation of a high performance Pt/SWCNT counter electrode for flexible dye-sensitized solar cells, Electrochimica Acta 56 (2011) 8545.
[36] M. Grätzel, Perspectives for dye-sensitized nanocrystalline solar cells, Prog. Photovoltaic Res. Applic. 8 (2000) 171.
[37] C. Kvarnstrom, H. Neugebauer, S. Blomquist, H. Ahonen, J. Kankare, A. Ivaska, N. Sariciftci, In situ FTIR spectroelectrochemical characterization of poly (3, 4-ethylenedioxythiophene) films, Synth. Met. 101 (1999) 66.
[38] P. Damlin, C. Kvarnstrom, A. Ivaska, Electrochemical synthesis and in situ spectroelectrochemical characterization of poly (3, 4-ethylenedioxythiophene) (PEDOT) in room temperature ionic liouids, J. Electroanal. Chem. 570 (2004) 113.
[39] M. Grätzel, Photoelectrochemical cells, Nature 414 (2001) 338.

[40] Y. Zhao, J. Zhai, T. Wei, L. Jiang, D. Zhu, Enhanced photoelectrical performance of TiO_2 electrodes integrated with microtube-network structures, J. Mater. Chem. 17 (2007) 5084.
[41] Y. Zhao, J. Zhai, J. He, X. Chen, L. Chen, L. Zhang, Y. Tian, L. Jiang, D. Zhu, High-performance all-solid-state dye-sensitized solar cells utilizing imidazolium-type ionic crystal as charge transfer layer, Chem. Mater. 20 (2008) 6022.
[42] B. Yoo, K. Kim, D. Lee, M. Ko, H. Lee, Y. Kim, W. Kimc, N. Park, Enhanced charge collection efficiency by thin-TiO_2-film deposition on FTO-coated ITO conductive oxide in dye-sensitized solar cells, J. Mater. Chem. 20 (2010) 4392.
[43] Y. Zheng, X. Tao, L. Wang, H. Xu, Q. Hou, W. Zhou, J. Chen, Novel ZnO-based film with double light-scattering layers as photoelectrodes for enhanced efficiency in dye-sensitized solar cells, Chem. Mater. 22 (2010) 928.
[44] M. Nazeeruddin, F. De Angelis, S. Fantacci, A. Selloni, G. Viscardi, P. Liska, S. Ito, B. Takeru, M. Grätzel, Combined experimental and DFT-TDDFT computational study of photoelectrochemical cell ruthenium sensitizers, J. Am. Chem. Soc. 127 (2005) 16835.
[45] H. Han, S. Lee, H. Shin, H. Jung, A quasi-inverse opal layer based on highly crystalline TiO_2 nanoparticles: a new light-scattering layer in dye-sensitized solar cells, Adv. Energy Mater. 1 (2011) 546.
[46] G. Mor, K. Shankar, M. Paulose, O. Varghese, C. Grimes, Use of highly-ordered TiO_2 nanotube arrays in dye-sensitized solar cells, Nano Lett. 6 (2006) 215.
[47] M. Nazeeruddin, A. Kay, I. Rodicio, R. Humphry-Baker, E. Mueller, P. Liska, N. Vlachopoulos, M. Graetzel, Conversion of light to electricity by cis-X_2 bis (2,2′-bipyridyl-4,4′-dicarboxylate) ruthenium (II) charge-transfer sensitizers ($X = Cl^-, Br^-, I^-, CN^-$ and SCN^-) on nanocrystalline TiO_2 electrodes, J. Am. Chem. Soc. 115 (1993) 6382.